

Fig. 6. Both the GC box and CRE are important for basal activity of the P22Ac promoter in H9c2 cells. *Left*, schematic representation of luciferase reporter constructs for the rat P22Ac promoter. Each luciferase reporter construct was generated as described under "Materials and Methods." A putative GC box site (-165) was mutated in Construct 2-MutG and 2-MutG&C. The CRE site (-26) was mutated in Construct 3-MutC and 2-MutG&C. Arrows show the transcription initiation site reported by Kitagawa *et al.* (23). *Right*, luciferase activity of the reporter constructs for the rat P22Ac promoter in H9c2 cells. The cells were transiently transfected with the P22Ac promoter-luciferase gene fusion plasmids. After 24 h of transfection, luciferase activity was assayed with cellular extracts as described under "Materials and Methods." Each value represents the mean of at least three independent experiments, and the S.D. was always within 10% of the mean.

Characterization of P22Ac Gene Promoter.—To investigate the mechanism of the transcriptional regulation of P22Ac expression, we used the 1.6-kb genomic fragment containing the promoter region of P22Ac inserted into a luciferase vector, pGL3 Basic. The transcriptional initiation site (nucleotide +1) was denoted in accordance with the report of Kitagawa *et al.* (23) (Fig. 6, arrows). The promoter region contains neither a TATA box nor a consensus CAAT sequence. The promoter region contains various transcription factor binding sites such as CRE at position -26, GC box for Sp1 (31) at positions -155 and -10, and binding sites for receptor-related orphan receptor α (ROR α) (32) at positions -778 and -553.

Both CRE and Sp1 Contribute to the Basal Expression of the P22Ac Gene.—In the report by Kitagawa *et al.* (23), a fragment of 118 bp (-162 to -44) was defined as the essential region for the gene expression of P22Ac. As shown in Fig. 6, the deletion fragments of the gene promoter were made from the HindIII-digested fragment (-1209 to +258, full-length) (Construct 1), and subcloned into a pGL3 Basic vector. Then, the activity of luciferase was assayed with the cells transfected with each deletion mutant vector. The activity was fully maintained in the 537-bp fragment (-279 to +258) (Construct 2), but it decreased to ~65% of the full activity in the 403-bp fragment (-145 to +258) (Construct 3) containing the CRE site. In the upstream fragment of 1064-bp (-1209 to -145) (Construct 6) containing the GC box, the activity decreased to ~40% of the full activity. However, the activity was almost lost in the upstream fragment of 1044-bp (-1209 to -165) (Construct 5) and the downstream fragment of 259 bp (-1 to +258) (Construct 4). The results indicated that the full promoter activity was located in the sequence between -278 and -1. To examine whether the CRE and GC box contribute to the full promoter activity, disabled mutants were generated for the consensus sequences of CRE at -26 and GC box at -155 in the luciferase vector containing the 537-bp Construct 2. In Construct 2-MutG



Fig. 7. Ca²⁺ modulators influence DNA binding to CRE in EMSA. H9c2 cells were incubated with thapsigargin (5 μ M) or BAPTA-AM (10 μ M) for the periods indicated, then the nuclear extracts were prepared as described under "Materials and Methods." ³²P-labeled oligonucleotide specific to CRE (-26) (A) and GC box (-155) (B) of the P22Ac gene promoter were prepared and incubated with each nuclear extract, and the binding was analyzed by EMSA. In *lane 7*, unlabeled oligonucleotide specific to CRE (-26) was added to the reaction mixture. In *lanes 8-10*, specific antibodies were added to the reaction mixture during the binding reaction for the supershift assay. C, quantitative data for the DNA binding to CRE and GC box shown in A and B. The intensity of gel-shift bands (arrows) was estimated densitometrically. Each value represents the mean of three experiments, and the S.D. was always within 10% of the mean.

binding activity involves both the CRE at -26 and GC box at -155, but it is specifically influenced by Ca²⁺ modulators, such as thapsigargin and BAPTA-AM, especially in the CRE at -26.

The Gene Promoter Activity of P22Ac Is Regulated by Ca²⁺ Modulators via CRE.—To confirm the CRE-dependent regulation of the gene expression of P22Ac by Ca²⁺ modulators, the gene promoter activity was examined by assaying the luciferase activity as described above. The cells were transfected with luciferase vector construct 3 (-145 to +258) (Fig. 6), which contains a CRE but no GC box. After 24 h of transfection, the cells were treated with 5 μ M thapsigargin or 10 μ M BAPTA-AM for predetermined periods, and the cell lysates were prepared and subjected to the assay for luciferase activity. As shown in Fig. 8A, the activity increased with thapsigargin to ~180% of the initial activity. The increase was not observed in the case of the disabled mutant for CRE with thapsigargin (data not shown). In contrast, with BAPTA-AM, the gene promoter activity decreased to ~85% of the initial level after 3 h of treat-

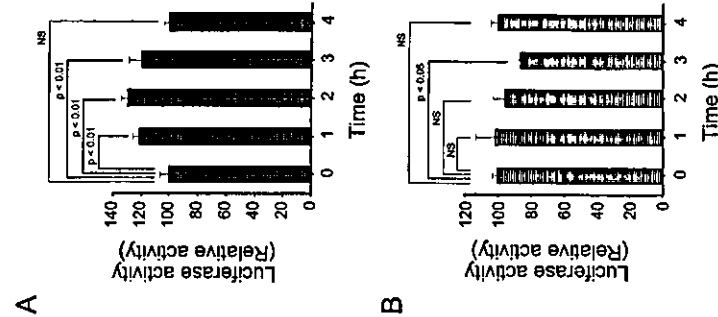


Fig. 8. Ca²⁺ modulators influence the promoter activity of the P22Ac gene in H9c2 cells. H9c2 cells were transiently transfected with luciferase vector construct 3 (-145 to +258) (Construct 3 in Fig. 6) containing CRE but no GC box. After 24 h of transfection, cells were treated with 5 μ M thapsigargin (A) or 10 μ M BAPTA-AM (B) for the periods indicated. Then luciferase activity was assayed with cell nuclear extracts as described under "Materials and Methods." Each value represents the mean \pm S.D. of at least three experiments. The statistical analysis was performed with a factorial analysis of variance test.

ment, but returned to the initial level after 4 h (Fig. 8B). In the disabled mutant of CRE (Construct 3-MutC in Fig. 6), the promoter activity was lost and no activity was observed even on treatment with thapsigargin or BAPTA-AM (data not shown). Collectively, the results indicate that the gene expression of P22Ac is transcriptionally regulated by the change of intracellular Ca²⁺ via CRE, and are consistent with the results of the EMSA for CRE binding (Fig. 6).

The Phosphorylation and Intracellular Localization of CREB Is Regulated by Ca²⁺ Modulators in H9c2 Cells.—CREB is a pivotal transcription factor for the regulation of cellular survival, and its activation is mediated by phosphorylation at a specific residue, Ser-133 (33). To investigate the effect of Ca²⁺ modulators on the phosphorylation status of CREB, the level of CREB phosphorylated at Ser-133 was examined by immunoblot analysis using specific antibodies in the cells treated with thapsigargin or BAPTA-AM. As shown in Fig. 9A, the phosphorylation level of CREB increased on treatment with thapsigargin.

NUCLEAR GLUTATHIONE S-TRANSFERASE π PREVENTS APOPTOSIS BY REDUCING THE OXIDATIVE STRESS-INDUCED FORMATION OF EXOCYCLIC DNA PRODUCTS

KENSAKU KAMADA,*¹ SHINJI GOTO,^{1,2} TOMOHIRO OKUNAGA,* YOSHITO IHARA,¹ KENTARO TSUI,¹ YOSHICHIKA KAWAI,^{1,2} KOJI UCHIDA,¹ TOSHIHIKO OSAWA,¹ TAKAYUKI MATSUO,*¹ IZUMI NAGATA,* and TAKAARITO KONDO¹

*Department of Neurology and ¹Department of Biochemistry and Molecular Biology in Disease, Atomic Bomb Disease Institute, Nagasaki University Graduate School of Biomedical Sciences, Nagasaki 851-8523, Japan; and ²Laboratory of Food and Biotechnology, Nagoya University Graduate School of Agricultural Sciences, Nagoya, Japan

(Received 7 June 2004; Revised 24 August 2004; Accepted 2 September 2004)

Available online 25 September 2004

Abstract—We previously found that nuclear glutathione S-transferase π (GST π) accumulates in cancer cells resistant to anticancer drugs, suggesting that it has a role in the acquisition of resistance to anticancer drugs. In the present study, the effect of oxidative stress on the nuclear translocation of GST π and its role in the protection of DNA from damage were investigated. In human colonic cancer HCT8 cells, the hydrogen peroxide (H₂O₂)-induced increase in nuclear condensation, the population of sub-G₁ peak, and the number of TUNEL-positive cells were observed in cells pretreated with edible mushroom lectin, an inhibitor of the nuclear transport of GST π . The DNA damage and the formation of lipid peroxide were dependent on the dose of H₂O₂ and the incubation time. Immunological analysis showed that H₂O₂ induced the nuclear accumulation of GST π but not of glutathione peroxidase. Formation of the 7-(2-oxo-heptyl)-substituted 1,N²-ethano-2'-deoxyguanosine adduct by the reaction of 13-hydroperoxyoctadecadienoic acid (13-HPODE) with 2'-deoxyguanosine was inhibited by GST π in the presence of glutathione. The conjugation product of 4-oxo-2-nonenal, a lipid aldehyde of 13-HPODE, with GSH in the presence of GST π was identified by LS/MS. These results suggested that nuclear GST π prevents H₂O₂-induced DNA damage by scavenging the formation of lipid-peroxide-modified DNA. © 2004 Elsevier Inc. All rights reserved.

Keywords—Oxidative stress, DNA damage, Glutathione S-transferase π , 7-(2-oxo-heptyl)-substituted 1,N²-ethano-2'-deoxyguanosine adduct, Free radical

INTRODUCTION

The role of oxidative stress as a mediator of apoptosis has been extensively studied. In particular, hydrogen peroxide (H₂O₂), a by-product of oxidative stress and a

Address correspondence to: Takahito Kondo, Department of Biochemistry and Molecular Biology in Disease, Atomic Bomb Disease Institute, Nagasaki University Graduate School of Biomedical Sciences, Nagasaki 851-8523, Japan; Fax: +81 (95) 849 7100; E-mail: kondo@med.nagasaki-u.ac.jp

¹ Contributed equally to this work.

² Present address: Department of Food Science, Graduate School of Nutrition and Biosciences, University of Tokushima, Japan.

1875

GST π ; it has been reported to accumulate in various human cancer tissues or precancer tissues and is employed in cancer research as a tumor marker [9–13]. An increase in GST π was also found in cancer cell lines resistant to doxorubicin hydrochloride (DOX), cis-diamminedichloroplatinum(II) (cisplatin: CDDP) [14–16], and alkylating agents [17].

In addition to its main location in the cytoplasm, GST π has been found in the nucleus in uterine cancer cells [18] and glioma cells [19]. These findings suggest a negative correlation between the existence of GST π in the nucleus of cancer cells and the survival of the patient. However, there has been no report on the mechanisms responsible for the nuclear survival of GST π or on the physiological role of nuclear GST π .

Edible mushroom lectin (*Agaricus bisporus* lectin; ABL) efficiently internalizes into the cytoplasm of cultured cells, localizes around the nucleus, and inhibits the nuclear transfer of proteins [20]. Previous reports presented evidence that ABL inhibits the nuclear transport of GST π and increases the sensitivity of cancer cells to anticancer drugs [21,22].

Endogenous lipid peroxidation products react with DNA and exocyclic DNA adducts to cause the covalent modification of nuclear bases [23,24]. During the lipid peroxidation process, lipid hydroperoxides are formed as the initial products, and the decomposition of the lipid hydroperoxides leads to the formation of aldehydes as the end products. Several aldehydes possess high reactivity against DNA bases, especially guanine [25–27]. Lipid-peroxide-induced DNA adduct formation and site-specific cleavage of double-stranded DNA have been reported [28,29]. Previously, Kawai *et al.* [30] studied the reaction of lipid hydroperoxides with DNA components and established a method to detect the formation of 7-(2-oxo-heptyl)-substituted 1,N²-ethano-2'-deoxyguanosine adducts (oxo-heptyl-edG) by the reaction of 13-hydroperoxyoctadecadienoic acid (13-HPODE) with 2'-deoxyguanosine (dG).

Recently, it was reported that 4-hydroxy-2-nonenal (4-HNE) and 4-oxo-2-nonenal (4-ONE), the end products of lipid peroxides, are nonenzymatically transferred to conjugate with GSH [31]. Moreover, 4-ONE, a major end product of 13-HPODE, had a higher affinity for the nucleus than 4-HNE. Even though it has been found that GST π catalyzes the formation of a conjugate of 4-HNE with GSH [32], its role in the formation of 4-ONE-GSH adducts was not known. In this study, we examined whether the nuclear GST π plays a role in the cellular sensitivity to oxidative stress caused by H₂O₂ and found that GST π prevents DNA damage by scavenging the oxo-heptyl-edG formed from 13-HPODE and forming a conjugate of 4-ONE with GSH.

MATERIALS AND METHODS

Materials

ABL was purchased from Wako Pure Chemical Industries Ltd. (Osaka, Japan), RPMI 1640 medium and fetal bovine serum (FBS) were obtained from Invitrogen Corp. (Carlsbad, CA). Sheep polyclonal antibodies against human glutathione peroxidase (GPX) were purchased from The Binding Site Ltd. (Birmmingham, UK), Horseradish peroxidase (HRP)-labeled anti-rabbit IgG, HRP-labeled anti-mouse IgG, and HRP-labeled anti-sheep IgG were from DAKO A/S (Glostrup, Denmark). The Enhanced Chemiluminescence (ECL) kit was obtained from Amersham Biosciences (Buckinghamshire, UK). All other chemicals and reagents were purchased from Sigma Aldrich (St. Louis, MO).

Preparation of cells

We used the human cancer cell lines HCT8 (colonic carcinoma) kindly donated by Dr. K. J. Scanlon. HCT8 cells were supplemented with 10% FBS at 37°C in 5% CO₂ with 100% humidity. Six hours before treatment with ABL, the cells were maintained in medium with 1% FBS. About 2 × 10⁶ cells were harvested with trypsin and washed with phosphate-buffered saline (0.137 M NaCl, 2.68 mM KCl, and 10 mM NAH₂PO₄/Na₂HPO₄, pH 7.4; PBS) twice at 4°C. The pellets were stored at –80°C before use.

TUNEL assay

The terminal deoxynucleotidyl transferase-mediated dUTP nick end labeling (TUNEL) assay was performed using an Apop Tag Plus Fluorescein in situ Apoptosis Detection Kit (Intergen Co., Purchase, NY). Briefly, approximately 2 × 10⁶ cells were harvested, fixed in 70% ethanol, treated with terminal deoxynucleotidyl transferase for 1 h and then fluorescein isothiocyanate (FITC) conjugate anti-digoxigenin for 1 h at room temperature, washed with 0.1% Triton X-100/PBS, and resuspended in propidium iodide containing RNase A. Fluorescence intensity was estimated simultaneously using a FACScan flow cytometer (Becton-Dickinson, San Jose, CA).

Nuclear condensation

For the histochemical analysis, HCT8 cells were maintained with RPMI 1640 medium containing 10% FBS in a four-well Lab Tec Chamber (Nalge Nunc International, Naperville, IL). After treatment with H₂O₂, cells were treated with 10 μ M Hoechst 33342 for 30 min to estimate the extent of nuclear condensation. They were then washed again with PBS. Fluorescence intensity was examined using an Axioskop2 fluorescence microscope (Carl Zeiss, Jena, Germany), and the findings were

analyzed using a charge-coupled device camera (AxioCam) and AxioVision software.

Analysis of double-stranded breaks of DNA

DNA damage was determined by flow cytometry, based on the formation of sub-G1 peaks of DNA as described by Gong et al. [33]. HCT8 cells were washed with PBS, fixed with 70% ethanol for 12 h at -20°C, and then centrifuged and further incubated with citrate-phosphate buffer (1 v of 0.1 M citric acid and 24 v of 0.2 M Na₂HPO₄) for 15 min at 25°C. The DNA content per nucleus was evaluated in a FACScan flow cytometer after the nuclei were stained with propidium iodide.

Preparation of proteins

The cytoplasmic and nuclear proteins were prepared as described by Digram et al. [34]. Proteins in the whole cells were prepared as described previously [35].

Preparation of antibodies

GST π was purified from human placenta, and polyclonal antibody against human GST π was obtained by immunizing rabbits as described previously [21]. The monoclonal antibody to Oxo-heptyl-edG was prepared as described previously [30].

Immunological estimation

Immunological levels of GST π in the cytoplasm and nucleus were estimated by Western blotting. Lysate from the extract of cells was separated by SDS-polyacrylamide gel electrophoresis (SDS-PAGE) in a 12.5% gel, transferred to a nitrocellulose membrane, and immunologically stained using rabbit IgG against human GST π or sheep IgG against human GPX as the primary antibody and HRP-labeled anti-rabbit IgG or

HRP-labeled anti-sheep IgG as the secondary antibody. Blots were developed by enhanced chemiluminescence using the ECL kit and the relative immunological activity was analyzed by NIH Image. The protein concentration was determined according to Redinbaugh and Tureley [36], with bovine serum albumin as the standard.

Estimation of lipid peroxide in the nucleus

Nuclei extracts were prepared as described by Abmayr and Wartman [37]. Nuclear thiobarbituric acid reactive substance (TBARS) levels were determined according to the method of Ohkawa et al. [38] using tetramethoxypropene (Wako Pure Chemical Industries).

Estimation of oxo-heptyl-edG

Cells incubated in various conditions were harvested with trypsin and washed with PBS two times at 4°C. The cells were then suspended in 10 mM citrate buffer (pH 6.0) and incubated for 10 min at 95°C. After a wash with PBS two times, the cells were suspended in 2 M HCl for 30 min at room temperature and rewashed with PBS two times. The levels of oxo-heptyl-edG in the cells were estimated by flow cytometry using anti-oxo-heptyl-edG mouse monoclonal antibody (mAb6A3) and FITC-conjugated anti-mouse IgG antibody.

Effect of GST π on the formation of oxo-heptyl-edG

13-HPODE (20 mM) was mixed with 1 mM FeCl₂ and stood for 12 h at 37°C. The solution (13-HPODE, 5 mM and FeCl₂, 0.2 mM, as a final concentration) was incubated with or without GSH (1 or 5 mM) and GST π (0.2 U) in the presence of 5 μ g of calf thymus DNA for 1 h at 37°C. Then 1 and 5 μ g of DNA extracted from the solution by ethanol precipitation

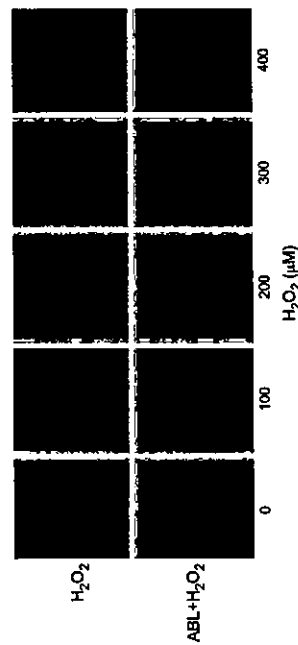


Fig. 1. Nuclear condensation. For the estimation of nuclear condensation, cells were incubated in a four-well Lab-Tec Chamber. After treatment with various concentrations of H₂O₂ for 24 h, cells were treated with 10 μ M Hoechst 33342 for 30 min for the estimation of nuclear condensation (top). The observation of fluorescence intensity was done using an Axiovert fluorescence microscope, and the findings were analyzed using a charge-coupled device camera and Axio Vision software. Cells were pretreated with ABL (40 μ g/ml) for 10 h and then treated with H₂O₂ (bottom).

were spotted on a nitrocellulose membrane and immunologically stained using MAb6A3 as the primary antibody and HRP-conjugated anti-mouse IgG antibody as the secondary antibody. Blots were developed by enhanced chemiluminescence using the ECL kit and the relative immunological activity was analyzed by NIH Image.

Liquid chromatography/mass spectrometry

The chemical structure of the product of the incubation of 4-ONE and GSH in the presence of GST π was characterized by liquid chromatography/mass spectrometry (LC/MS). The LC/MS was conducted using a Platform II (VIG Biotech) in an electrospray ionization positive (ESP+) mode. The gradient condition (solvent A, 0.01% trifluoroacetic acid; solvent B, acetonitrile containing 0.01% trifluoroacetic acid) was as follows: 100% A (0 min), 50% B (20 min), 100% B (30 min), 100% B hold (30–35 min), 100% A (40 min).

Statistical analysis

Data are presented as the mean \pm SD. Differences were examined using a Student *t* test. A value of *p* < 0.05 was considered significant.

RESULTS

Nuclear condensation

Nuclear condensation is a characteristic of apoptosis. The nuclear condensation caused by H₂O₂ was estimated morphologically using Hoechst 33342 (Fig. 1). Human colonic cancer HCT8 cells were incubated with various concentrations of H₂O₂ for 24 h. No DNA condensation was observed (100–400 μ M H₂O₂). ABL, a mushroom lectin, inhibits the nuclear transfer of GST π [1]. The cells were previously treated with 40 μ g/ml of ABL for 10 h and further incubated with H₂O₂ for 24 h. Nuclear condensation was observed in

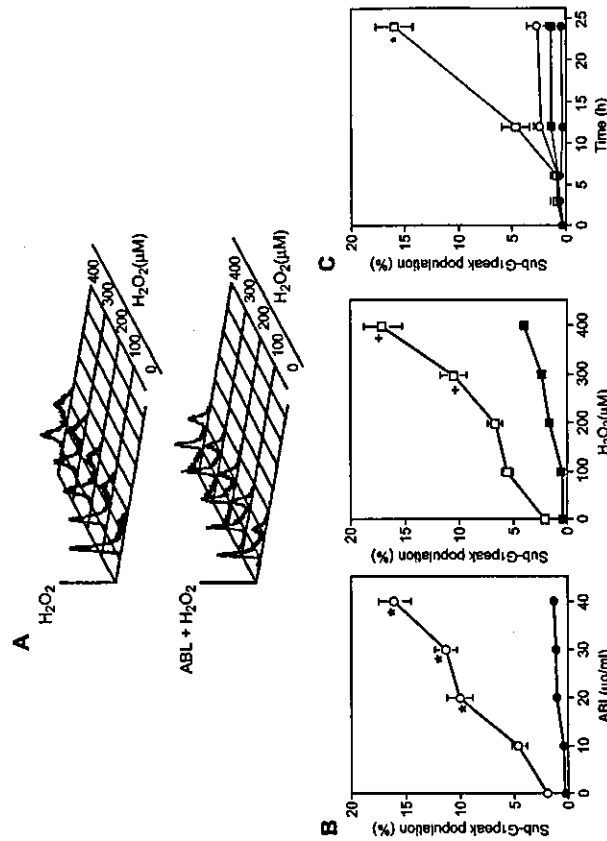


Fig. 2. Flow cytometric analysis of the DNA damage. (A) Effect of H₂O₂ on the DNA damage was analyzed using a FACScan flow cytometer. The sub-G₁ peak was estimated as a marker of the double-strand break of DNA. Treatment of cells with H₂O₂ or pretreatment with ABL was performed as described in Fig. 1 legend. (B) Effect of various concentrations of ABL (left) and H₂O₂ (right) on the formation of the sub-G₁ peak (%). C400 μ M H₂O₂ (+); 8H₂O₂ (-); 400 μ M ABL (+); 8ABL (-). **p* < 0.05 compared with cells without H₂O₂ treatment. †*p* < 0.05 compared with cells without ABL pretreatment. (C) Effect of incubation time on the formation of the sub-G₁ peak (%). C400 μ M H₂O₂ (+); 8H₂O₂ (-); 400 μ M ABL (+); 8ABL (-). **p* < 0.05 compared with H₂O₂-treated cells. Data are the means of three independent analyses. Bars show the SD.

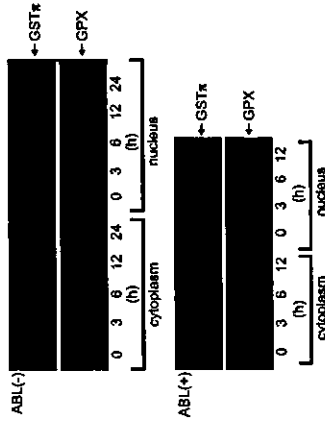


Fig. 4. Immunological estimation of the amount of GST π in the cytoplasm and nucleus. Proteins prepared from cellular cytoplasm and nucleus (1×10^7 cells) were separated by SDS-PAGE in a 12.5% gel transferred to a nitrocellulose membrane and immunologically stained using rabbit IgG or sheep IgG antibody against human GST π or GPX. Cells were treated with 400 μ M H₂O₂ for the period indicated with (bottom) or without (top) pretreatment with ABL for 10 h.

ABL increases the sensitivity of cells to H₂O₂, leading to DNA damage and apoptosis.

Immunological estimation of nuclear GST π

The amount of GST π induced by H₂O₂ was estimated. Fig. 4 shows results of Western blotting for GST π . H₂O₂ increased the levels of cytoplasmic GST π in a time-dependent manner (top). A concomitant increase in the level of GST π was observed in the nucleus. The effect of ABL on the nuclear transfer of GST π was studied (bottom). The H₂O₂-induced transfer of GST π to the nucleus was inhibited by ABL. The results were consistent with previous data [21].

In the cytoplasm, H₂O₂ is detoxified to H₂O by GPX. Then, the immunological activity of GPX was estimated (Fig. 4). Treatment with H₂O₂ increased the levels of GPX in the cytoplasm. During the experiment, no GPX was transferred to the nucleus. Similarly, the immunological activity of glutathione reductase was not found in the nucleus in the presence or absence of H₂O₂ (data not shown).

Estimation of lipid peroxide in the nucleus

The formation of lipid peroxides was determined as the TBARS levels (Fig. 5). H₂O₂ increased the levels of nuclear TBARS when the cells were pretreated with ABL.

Role of nuclear GST π

Kawai *et al.* [30] reported that DNA bases are modified with lipid peroxide of linoleic acids leading to DNA damage. 4-ONE is nonenzymatically formed from 13-HPODE, which reacts with dG to form oxo-heptyl-eG. Doorn and Petersen [31] reported that 4-ONE has a higher affinity for nucleotides than 4-HNE and, on the other hand, spontaneously reacts with GSH to form its GSH conjugate [31]. We then speculated that

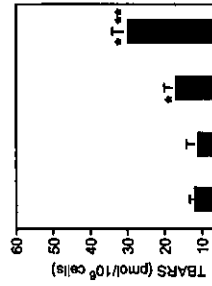


Fig. 5. Estimation of lipid peroxide in the nucleus. The formation of the nuclear TBARS was determined using tetraethoxypropene. Data are the means of three independent analyses. Bars show the SD. **p* < 0.05 compared with control cells. ***p* < 0.05 compared with H₂O₂-treated cells.

a manner dependent on the dose of H₂O₂, when the cells were pretreated with ABL. These results suggest that inhibition of the nuclear transfer of GST π by ABL enhanced the H₂O₂-induced DNA damage.

Effect of H₂O₂ on DNA damage

To understand the extent of the DNA damage by H₂O₂, the sub-G₁ peak was estimated flow cytometrically as a marker of the double-stranded breaks of DNA (Fig. 2A). The DNA damage induced by pretreatment with ABL was not apparent (Fig. 2B, left) and damage was slightly induced by H₂O₂ alone (Fig. 2B, right). ABL increased the population of the sub-G₁ peak induced by 400 μ M H₂O₂ in a dose-dependent (10–40 μ g/ml) manner (Fig. 2B, left). Pretreatment with 40 μ g/ml of ABL for 10 h enhanced the population of the sub-G₁ peak induced by H₂O₂ (100–400 μ M) for 24 h dose dependently (Fig. 2B, right). The effect of ABL on the H₂O₂-induced DNA damage was dependent on the incubation time with H₂O₂ (Fig. 2C). These results suggest that ABL increases the sensitivity of cells to H₂O₂.

TUNEL assay

The H₂O₂-induced DNA damage was also estimated by TUNEL assay (Fig. 3). At 400 μ M H₂O₂ increased the proportion of TUNEL-positive cells in 12 h (10%) with a subsequent decrease at 24 h (5%). Pretreatment with ABL (40 μ g/ml) caused an increase in TUNEL-positive cells induced by 400 μ M H₂O₂, 28% in 12 h and 42% in 24 h (Figs. 3A and 3B). These results also suggest that

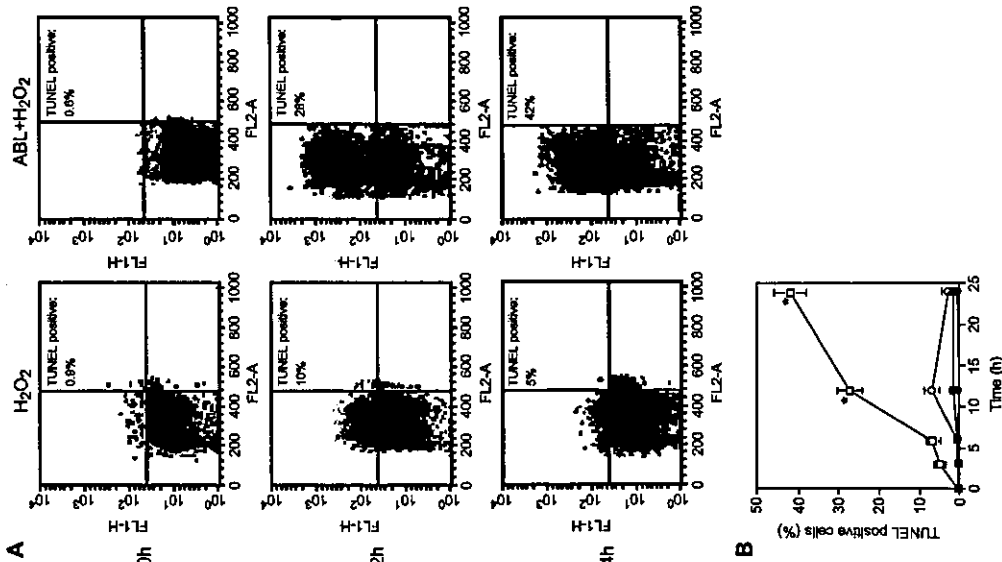


Fig. 3. TUNEL assay. The effect of ABL on the cytotoxicity of H₂O₂ was examined by TUNEL assay using an Apop Tag Plus Fluorescein In Situ Apoptosis Detection Kit as described under Materials and methods. (A) Cells (2×10^7) treated with 400 μ M H₂O₂ for 12 and 24 h (left) or pretreated with ABL (40 μ g/ml) for 10 h (right). (B) Effect of incubation time on the TUNEL-positive cells (%). O: 400 μ M H₂O₂; ●: control; ◐: 400 μ M H₂O₂ with ABL pretreatment. Data are the means of three independent analyses. Bars show the SD. **p* < 0.05 compared with H₂O₂-treated cells.

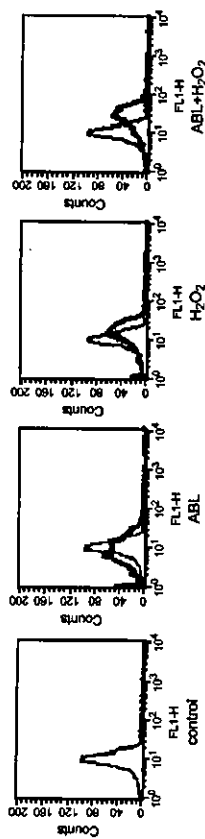


Fig. 6. Immunological estimation of oxo-heptyl-edG. Effects of ABL (panel 2), H₂O₂ (panel 3), and H₂O₂ with ABL pretreatment (panel 4) on the levels of oxo-heptyl-edG in the cells were estimated by flow cytometer using anti-oxo-heptyl-edG mouse monoclonal antibody (mAb6A3) and FITC-conjugated anti-mouse IgG antibody.

human GST π catalyzed the formation of 4-ONE conjugated with GSH, which can then prevent the DNA from being modified with lipid peroxide. The immunological activity of lipid-peroxide-modified DNA was estimated flow cytometrically using anti-oxo-heptyl-edG. The formation of oxo-heptyl-edG was observed following treatment with 400 μ M H₂O₂ for 12 h (Fig. 6, panel 3) and increased on pretreatment with ABL (Fig. 6, panel 4). The possible role of GST π in preventing the formation of lipid peroxide-DNA was affirmed *in vitro*. A mixture of 13-HPODE and FeCl₃ stood for 12 h at 37°C. The mixture was incubated with calf thymus DNA for 1 h at 37°C in the presence or absence of 5 mM GSH and 0.2 U of GST π . The formation of oxo-heptyl-edG was estimated from immuno blots (Fig. 7). The formation of oxo-heptyl-edG was inhibited by 20% in the presence of GSH (Fig. 7, lane 2) and by 60% in the presence of GST π and GSH (Fig. 7, lane 4). The results suggest that GST π inhibits the formation of oxo-heptyl-edG in the nucleus. Fig. 8 shows the results of LC/MS measurements of the adduct formation of 4-ONE and GSH in the presence or absence of GST π . In the absence of GST π , the LC/MS analysis of the product gave a pseudomolecular ion peak [M + H]⁺ at *m/z* 462 (Fig. 8B). In the presence of GST π , this value apparently increased (Fig. 8C). Since the possible molecular weight of the ONE-GSH adduct is 641.18 (Fig. 9), the data obtained by LC/MS support the idea that GST π catalyzes the formation of the product.

DISCUSSION

In this study, we found for the first time that nuclear GST π functions to scavenge lipid-peroxide-induced DNA damage. We showed that (1) hydrogen peroxide increased the modification of nuclear DNA induced by lipid peroxide to cause DNA damage followed by the induction of apoptosis, (2) the nuclear GST π prevented DNA damage from lipid peroxide by scavenging the oxo-heptyl-edG formed by the reaction of 13-HPODE with edG (the product of the conjugation of 4-ONE, one of the

major breakdown products of 13-HPODE, with GSH catalyzed by GST π was identified), and (3) ABL inhibited the nuclear transfer of GST π to increase the sensitivity of the nucleus to oxidative stress. These findings suggest that nuclear GST π prevents H₂O₂-induced DNA damage by scavenging lipid-peroxide-modified DNA.

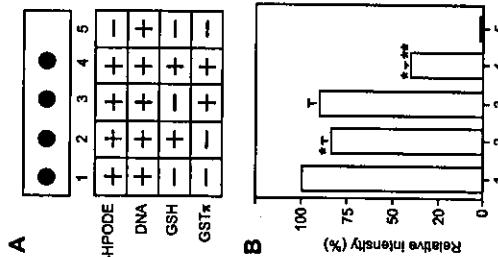


Fig. 7. Effect of GST π on the formation of oxo-heptyl-edG *in vitro*. (A) 13-HPODE was mixed with FeCl₃ and stood for 12 h at 37°C. The solution was incubated with or without GSH and GST π in the presence of calf thymus DNA for 1 h at 37°C. DNA extract was spotted on a nitrocellulose membrane and immunologically stained using mAb6A3 as the primary antibody and HRP-conjugated anti-mouse IgG antibody as the secondary antibody. Blots were developed by enhanced chemiluminescence using the ECL kit and the relative immunological activity was analyzed by NIH image. (B) Relative intensity (%) of the levels of oxo-heptyl-edG in each lane corresponds to A. Data are the means of three independent analyses. Bars show the SD. **p* < 0.05 compared with control cells; ***p* < 0.05 compared with H₂O₂-treated cells.

present study, H₂O₂-induced DNA damage was observed when the cells were previously treated with ABL, an inhibitor of the nuclear transfer of GST π (Figs. 1-3). Strikingly, HCT8 cells were not sensitive to H₂O₂ (~400 μ M). Treatment of the cells with H₂O₂ increased the nuclear transfer of GST π in a dose- (data not shown) and time-dependent manner (Fig. 4). The resistance of HCT8 cells to oxidative stress was abolished by pretreatment with ABL. The results strongly suggest an important role for the nuclear GST π in the sensitivity of the cells to oxidative stress.

There are many antioxidants in cells. Most of them are localized in the cytoplasm. In addition, each microorganism possesses its own defense system against oxidative stress. A nuclear superoxide dismutase, GPX, and GST π have been reported [21,39,40].

Adler *et al.* [41] reported that GSTp associates with Jun N-terminal kinase (JNK) to regulate its activity in mouse fibroblast NIH3T3 cells. Moreover, Yin *et al.* [42] demonstrated that GSTp coordinates the activation of extracellular signal-regulated kinases/p38 mitogen-activated protein kinase/inhibitor of κ kinase and suppression of JNK as part of the mechanism underlying its ability to elicit protection against H₂O₂-induced cell death. These findings indicate that GSTp plays an important role in the defense system against oxidative stress through its function as a regulator of stress kinases. It is interesting that GSTp has at least two different functions, to scavenge lipid peroxide and to regulate stress kinases as an antioxidant.

Lipid hydroperoxides are known to be relatively short lived. They are enzymatically and/or nonenzymatically metabolized to stable alcohols *in vivo*. They also react with metal to form reactive end products

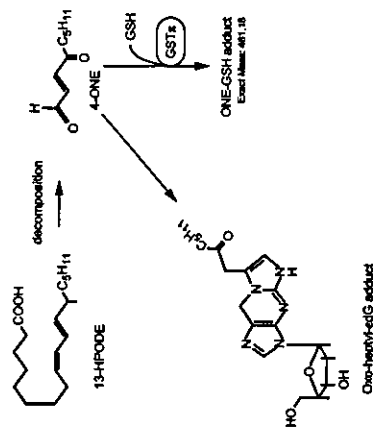


Fig. 9. Schema of the metabolism of 13-HPODE in the nucleus.

Fig. 8. LC/MS analysis. The chemical structure of the product of the incubation of 13-HPODE and GSH in the presence or absence of GST π was characterized by LC/MS. Materials were prepared as described in Fig. 6 legend. (A) 13-HPODE; (B) 13-HPODE with GSH; (C) 13-HPODE with GSH and GST π . Arrow indicates 4-ONE-GSH adduct.

Previously, we found that the nuclear GST π is an important factor in the acquisition of drug resistance in cancer cells [21,22]. Cancer cells which expressed the nuclear GST π in response to anticancer drugs such as DOX and CDDP showed resistance to these drugs, whereas the cells that did not express nuclear GST π were more sensitive to the drugs. The conjugation of the drugs with GSH was found in the resistant cells and correlated with decreased drug-induced DNA damage. In the

- such as aldehydes. However, the importance of lipid hydroperoxides to the covalent modifications of biological components has not been thoroughly investigated. oxo-heptyl-eG is formed by the reaction of 13-HPODE with eG [43]. During this reaction, 4-ONE directly mediates the formation of oxo-heptyl-eG [30,43], suggesting that the lipid-hydroperoxide-derived production of 4-ONE contributes to DNA damage. 4-ONE and 4-HNE also form adducts with proteins. These adducts of proteins and DNA are thought to be involved in the pathogenesis of several diseases such as atherosclerosis [44], diabetes mellitus [45], and carcinogenesis [30].
- With regard to the reduction of lipid peroxide, reduction of linoleic acid hydroperoxide by GPX was reported [46]. Lipid peroxide once formed is reduced to alcohol by GPX. With regard to the role of GST in the reduction of lipid peroxide, Cao *et al.* [32] reported that GSH and GST function in protecting against the cytotoxicity of 4-HNE in vascular smooth muscle cells. Depletion of GSH by buthionine sulfoximine and inhibition of GST activity by sulfasalazine potentiated the 4-HNE-mediated cytotoxicity. The results suggested that GST functions to form a conjugate of 4-HNE with GSH.
- Zimniak *et al.* [47] reported that mouse GSTA4-4 belongs to the alpha subclass of GST and functions to form a conjugate of 4-HNE with GSH. Additionally, Singhal *et al.* [48] reported that the human GST corresponding to mouse GSTA4-4 catalyzes the conjugation of 4-HNE with GSH. These reports indicate that GSTA4-4 plays an important role with GSH in the removal of 4-HNE. It is possible that GSTA4-4 functions to form a conjugate of 4-ONE with GSH. On the other hand, the colon cancer cell line employed in the present study possessed mainly GST π , which may detoxify 4-HNE and 4-ONE. It has been reported that aldose reductase prevents the formation of 4-HNE [49]. However, there has been no report on the role of GST in the reduction of another lipid peroxidation product, 4-ONE. As shown in Fig. 9, this is the first report to show that GST π reduces the formation of DNA adducts with 13-HPODE, characterized as oxo-heptyl-eG. GST π catalyzes the conjugation of 4-ONE, a lipid-peroxide-derived product, with GSH, the adduct of which is thought to contribute to age-related diseases or carcinogenesis.
- Acknowledgments*—We are very grateful to Ms. Junko Takasaki for preparing the manuscript. This work was supported in part by Grants-in-Aid for Scientific Research from the Ministry of Education, Science, Sports, and Culture of Japan.
- REFERENCES**
- [1] Kaneto, H.; Fujii, J.; Suzuki, K.; Kasai, H.; Kawamura, F.; Kamada, T.; Tsuniguchi, N. DNA cleavage induced by glyoxal and Cu,Zn-superoxide dismutase. *Biochem. J.* 304:219–225, 1994.
 - [2] Nosa, K.; Shibayama, M.; Kikuchi, K.; Kageyama, H.; Saitayama, T.; Kuroki, T. Transcriptional activations of early-response genes by hydrogen peroxide in a mouse osteoblastic cell line. *Eur. J. Biochem.* 201:99–106, 1991.
 - [3] Jacoby, W. B. The glutathione S-transferase: a group of multifunctional detoxification proteins. *Adv. Enzymol. Relat. Areas Mol. Biol.* 46:383–414, 1978.
 - [4] Chasseaud, L. F. The role of glutathione and glutathione S-transferase in the metabolism of chemical carcinogens and other electrophilic agents. *Adv. Cancer Res.* 29:175–274, 1979.
 - [5] Probst, J. R.; Gaudier, H. E. Glutathione peroxidase activity of glutathione S-transferases purified from rat liver. *Biochem. Biophys. Res. Commun.* 76:437–445, 1977.
 - [6] Meyer, D. J.; Beale, D.; Tan, K. H.; Coles, B.; Ketterer, B. Glutathione transferases in primary rat hepatomas: the isolation of a form with GSH peroxidase activity. *FEBS Lett.* 184:139–143, 1985.
 - [7] Tan, K. H.; Meyer, D. J.; Coles, B.; Ketterer, B. Thymine hydroperoxide: a substrate for rat Se-dependent glutathione peroxidase and glutathione transferase isoenzymes. *FEBS Lett.* 307:231–233, 1986.
 - [8] Ujihara, M.; Tachibana, S.; Sutoh, K.; Sato, K.; Utsuki, Y. Biochemical and immunological demonstration of prostaglandin D₂ 5 α and F₂ formation from prostaglandin H₂ by various rat glutathione S-transferase isoenzymes. *Arch. Biochem. Biophys.* 264:428–437, 1988.
 - [9] Sato, K.; Kitahara, A.; Soma, Y.; Inaba, Y.; Hatanaka, I.; Sato, K. Purification, induction, and distribution of placental glutathione transferase: a new marker enzyme for preneoplastic cells in the rat chemical hepatocarcinogenesis. *Proc. Natl. Acad. Sci. USA* 81:3964–3968, 1984.
 - [10] Kano, T.; Sakai, M.; Muramatsu, M. Structure and expression of a human class α glutathione S-transferase messenger RNA. *Cancer Res.* 47:5636–5639, 1987.
 - [11] Hennink, B.; Castro, V. M.; Danielson, U. H.; Tahir, M. K.; Huisman, J.; Ringborg, U. Expression of class II glutathione transferase in human malignant melanoma cells. *Carcinogenesis* 8:1979–1982, 1987.
 - [12] Howie, A. F.; Forrester, L. M.; Glazebrook, J. S.; Schlager, J. J.; Powis, G.; Beckert, G. J.; Hayes, J. D.; Wolf, C. R. Glutathione transferase and glutathione peroxidase expression in normal and tumour human tissues. *Carcinogenesis* 11:451–458, 1990.
 - [13] Hirata, S.; Oajima, T.; Kohana, G.; Ishigaki, S.; Nizma, Y. Significance of glutathione S-transferase- α as a tumor marker in patients with oral cancer. *Cancer* 70:2381–2387, 1992.
 - [14] Sakai, Y.; Nakayama, M.; Ono, M.; Sakai, M.; Muramatsu, M.; Kohno, K.; Kuwano, M. Increased expression of glutathione S-transferase gene in sit-dimethylnitrosobenzimidazole-resistant variants of a Chinese hamster ovary cell line. *Cancer Res.* 49:7020–7025, 1989.
 - [15] Bai, F.; Nakamichi, Y.; Kawasumi, M.; Takayama, K.; Yasunami, J.; Ito, X. H.; Tamura, N.; Watanabe, K.; Hirai, N. Immunohistochemical expression of glutathione S-transferase-I α can predict chemotherapeutic response in patients with non-small cell lung carcinoma. *Cancer* 78:416–421, 1996.
 - [16] Baint, G.; Jhupia, A.; Shaha, B. K.; Kati, A. G.; Myers, C. E.; Cowan, K. H. Overexpression of a novel anionic glutathione transferase in multidrug-resistant human breast cancer cells. *J. Biol. Chem.* 261:15544–15549, 1986.
 - [17] Wang, Y. Y.; Teicher, B. A.; Shea, T. C.; Holden, S. A.; Rebb, K. W.; al-Ash, A.; Hamner, W. D. Cross-resistance and glutathione S-transferase- π levels among four human melanoma cell lines selected for alkylating agent resistance. *Cancer Res.* 49:6185–6192, 1989.
 - [18] Shiratori, Y.; Soma, Y.; Maruyama, H.; Sato, S.; Takano, A.; Sato, K. Immunohistochemical detection of the placental form of glutathione S-transferase in dysplastic and neoplastic human uterine cervix lesions. *Cancer Res.* 47:6806–6809, 1987.
 - [19] Ali-Osman, F.; Brunner, J. M.; Kuhlth, T. M.; Hess, K. Propagative significance of glutathione S-transferase α expression and subcellular localization in human gliomas. *Clin. Cancer Res.* 3:2253–2261, 1997.
 - [20] Yu, L. G.; Fenig, D. G.; White, M. R. H.; Spiller, D. G.; Appleton, P.; Evans, R. C.; Gronow, I.; Smith, J. A.; Davies, H.; Gieremek, O. V.; Paterson, O. H.; Milton, J. D.; Rhodes, J. M. Edible mushroom (*Agaricus bisporus*) lectin, which reversibly inhibits epithelial cell proliferation, blocks nuclear localization sequences-dependent nuclear protein import. *J. Biol. Chem.* 274:4890–4899, 1999.
 - [21] Goto, S.; Ibara, Y.; Ura, Y.; Izumi, S.; Ake, K.; Koji, T.; Kondo, T. Doxorubicin-induced DNA intercalation and carcinogenicity by nuclear glutathione S-transferase π . *FASEB J.* 14:2702–2714, 2000.
 - [22] Goto, S.; Kamei, K.; Sak, Y.; Ibara, Y.; Kondo, T. Significance of nuclear glutathione S-transferase π in responses to anti-cancer drugs. *Jpn. J. Cancer Res.* 91:047–1056, 2002.
 - [23] Burcham, P. C. Genotoxic lipid peroxidation products: their DNA damaging properties and role in formation of endogenous DNA adducts. *Mutagenesis* 13:287–303, 1998.
 - [24] Manetti, L. J. Lipid hydroperoxide-DNA damage by malondialdehyde. *Mutat. Res.* 424:93–95, 1999.
 - [25] Sato, H.; Okada, T.; Takemura, T.; Ikemura, T. Reaction of malondialdehyde with nucleic acid. I. Formation of fluorescent pyrimidyl(2'-alanyl)-10 (3H)-one nucleosides. *Bull. Chem. Soc. Jpn.* 56:1799–1802, 1983.
 - [26] Winter, C. K.; Segall, H. J.; Hadden, W. F. Formation of cyclic adducts of deoxyguanosine with the aldehydes *trans*-4-hydroxy-2-hexenal and *trans*-4-hydroxy-2-nonenal in vitro. *Cancer Res.* 46:5682–5686, 1986.
 - [27] Chung, F.-L.; Young, R.; Hsieh, S. S. Formation of cyclic 1, N⁶-propanodeoxyguanosine adducts in DNA upon reaction with acrolein or crotonaldehyde. *Cancer Res.* 44:990–995, 1984.
 - [28] Wang, M.-Y.; Lieber, J. G. Lipid hydroperoxide-induced endogenous DNA adducts in hamsters: possible mechanism of lipid hydroperoxide-mediated carcinogenesis. *Arch. Biochem. Biophys.* 316:38–46, 1995.
 - [29] Inoue, S. Site-specific cleavage of double-stranded DNA by hydroperoxide of linoleic acid. *FEBS Lett.* 174:231–234, 1984.
 - [30] Kawai, Y.; Kato, Y.; Nakae, D.; Kamada, O.; Konishi, Y.; Uchida, K.; Otsu, T. Immunohistochemical detection of a substituted 1,N⁶-ethanodeoxyguanosine adduct by α -9-polyaminomethyl acid hydroperoxide in the liver of rats fed a choline-deficient, L-amino acid-defined diet. *Carcinogenesis* 3:485–489, 2002.
 - [31] Dunn, J. A.; Petersen, D. R. Covalent adduction of nucleophilic amino acids by 4-hydroxyhexenal and 4-oxononenal. *Chem. Biol. Interact.* 114:3–144, 91–100, 2003.
 - [32] Cao, Z.; Haged, D.; Trombetta, L. D.; Li, Y. The role of chemically induced glutathione and glutathione S-transferase in protecting against 4-hydroxy-2-nonenal-mediated cytotoxicity in vascular smooth muscle cells. *Cardiovasc. Toxicol.* 3:165–177, 2003.
 - [33] Gong, J.; Taganov, F.; Daryzkiwicz, Z. A. Selective procedure for DNA extraction from apoptotic cells applicable for gel electrophoresis and flow cytometry. *Anal. Biochem.* 218:314–319, 1994.
 - [34] Dignam, J. D.; Lebovitz, R. M.; Roeder, R. G. Accurate transcription initiation by RNA polymerase II in a soluble extract from isolated mammalian nuclei. *Nucleic Acids Res.* 11:1475–1489, 1983.
 - [35] Goto, S.; Iida, T.; Cho, S.; Oka, M.; Kohno, S.; Kondo, T. Overexpression of glutathione S-transferase α enhances the adhesion formation of capillaries with glutathione in human cancer cells. *Free Radic. Res.* 31:549–558, 1999.
 - [36] Redinbaugh, M. G.; Turley, R. B. Adaptation of the bicinchoninic acid protein assay for use with microtiter plates and microgradient fractionation. *Anal. Biochem.* 152:267–271, 1986.
 - [37] Atanasi, S. M.; Watanabe, J. I. DNA-protein interactions. In: *Antioxid. F. M.; Breat, R. J.; Kingston, R. E.; Moore, D. D.; Seidman, J. G.; Smith, J. A.; Strub, K., eds. Current protocols in molecular biology*. Vol. 11. New York: Current Publishing Associates and Wiley-Interscience, 1203–1219, 1987.
 - [38] Ohtsuka, H.; Ohishi, N.; Yagi, K. Assay for lipid peroxide in animal tissues by thiobarbituric acid reaction. *Anal. Biochem.* 95:351–358, 1979.
 - [39] Ohtsuka, T.; Kizaki, T.; Takayama, E.; Izumi, N.; Matsubara, O.; Iwata, Y.; Suzuki, K.; Li, J. L.; Takayama, T.; Tsuniguchi, N.; Ohno, H. Nuclear translocation of extracellular superoxide dismutase. *Biochem. Biophys. Res. Commun.* 296:54–61, 2002.
 - [40] Nakamura, T.; Inai, H.; Tamashima, N.; Nakagawa, Y. Molecular cloning and functional expression of nuclear polyphospholipid hydroperoxide glutathione peroxidase in mammalian cells. *Biochem. Biophys. Res. Commun.* 311:139–148, 2003.
 - [41] Adley, Y.; Yin, Z.; Fuchs, S. Y.; Benezra, M.; Rosario, L.; Tew, K. D.; Pucina, M. R.; Sarda, M.; Henderson, C. J.; Wolf, C. R.; Davis, R. J.; Ronai, Z. Regulation of JNK signaling by GST π . *EMBO J.* 18:1321–1334, 1999.
 - [42] Yin, Z.; Vladimir, N. I.; Hasen, H.; Koneth, T.; Ronai, Z. Glutathione S-transferase π elicits protection against H₂O₂-induced cell death via coordinated regulation of stress kinases. *Cancer Res.* 60:4054–4057, 2000.
 - [43] Kung'u, D.; Nakajima, M.; Wehrli, S.; Xu, K.; Blair, I. A. Covalent modifications to Z'-deoxyguanosine by 4-oxo-2-nonenal, novel product of lipid peroxidation. *Chem. Res. Toxicol.* 12:1195–1204, 1999.
 - [44] Rosenfeld, M. E.; Palinski, W.; Yin-Fernandez, S.; Butler, S.; Witzman, J. L. Distribution of oxidation specific lipid protein adducts and apolipoprotein B in atherosclerotic lesions of varying severity from WHHL rabbits. *Atherosclerosis* 103:336–349, 1993.
 - [45] Yamauchi, J.; Takano, A.; Itagaki, S.; Kawamura, S.; Yoshitani, Y. APA baxeter model for diabetic atherosclerosis. 2. Analysis of lipids and lipoproteins. *Exp. Anim.* 42:267–274, 2000.
 - [46] Little, C.; O'Brien, P. J. An intracellular GSH-peroxidase with a lipid hydroperoxide substrate. *Biochem. Biophys. Res. Commun.* 31:145–150, 1968.
 - [47] Zimniak, P.; Singhal, S. S.; Srivastava, S. K.; Awasthi, S.; Sharma, R.; Hyun, J. B.; Awasthi, Y. C. Estimation of genomic complexity, heterologous expression, and enzymatic characterization of mouse glutathione S-transferase mGSTA4-4 (GST5.7). *J. Biol. Chem.* 269:992–1000, 1994.
 - [48] Singhal, S. S.; Zimniak, P.; Awasthi, S.; Piper, J. T.; Ha, N. G.; Teng, J. J.; Petersen, D. R.; Awasthi, Y. C. Several closely related glutathione S-transferase isozymes catalyzing conjugation of 4-hydroxyhexenal are differentially expressed in human tissues. *Arch. Biochem. Biophys.* 311:242–250, 1994.
 - [49] Vander Jagt, D. L.; Kolb, N. S.; Vander Jagt, T. J.; Chino, J.; Martinez, F. J.; Hunsaker, L. A.; Rorer, R. E. Substrate specificity of human aldose reductase: identification of 4-hydroxyhexenal as an endogenous substrate. *Biochim. Biophys. Acta* 1249:117–126, 1995.

Functional variation in *LGALS2* confers risk of myocardial infarction and regulates lymphotoxin- α secretion *In vitro*

Kojiro Ozaki¹, Kazumi Inoue², Hiroaki Sato³, Akiaki Ito⁴, Yoko Ohmaki¹, Akiko Sakano⁵, Hiroyuki Sato⁶, Kenta Okabe¹, Masahito Kobayashi¹, Masahito Mori¹, Yasuko Mizumoto^{1,5} & Toshihiro Taniguchi¹

¹Laboratory for Cardiovascular Diseases, SNP Research Center, The Institute of Physical and Chemical Research (RIKEN), Tokyo 108-8639, Japan
²Department of Cardiology, Kokura Memorial Hospital, Kitakyushu 802-8555, Japan
³Department of Internal Medicine and Therapeutics, Osaka University Graduate School of Medicine, Suita 565-0871, Japan
⁴Laboratory for Genotyping, SNP Research Center, The Institute of Physical and Chemical Research (RIKEN), Yokohama 230-0045, Japan
⁵Laboratory of Molecular Medicine, Human Genome Center, Institute of Medical Science, University of Tokyo, Tokyo 108-8639, Japan

Myocardial infarction (MI) has become one of the leading causes of death in the world. Its pathogenesis includes chronic formation of plaque inside the vessel wall of the coronary artery and acute rupture of the artery, implicating a number of inflammation-mediated molecules, such as the cytokine lymphotoxin- α (LTA). Functional variations in *LTA* are associated with susceptibility to MI. Here we show that *LTA* protein binds to galectin-2, a member of the glucose-binding lectin family. Our case-control association study in a Japanese population showed that a single nucleotide polymorphism in *LGALS2* encoding galectin-2 is significantly associated with susceptibility to MI. This genetic substitution affects the transcriptional level of galectin-2 *in vitro*, potentially leading to altered secretion of LTA, which would then affect the degree of inflammation; however, its relevance to other populations remains to be clarified. Smooth muscle cells and macrophages in the human atherosclerotic lesions expressed both galectin-2 and LTA. Our findings thus suggest a link between the *LTA* cascade and the pathogenesis of MI.

To understand better the role of LTA in the pathogenesis of this disease, we searched for proteins that interact with LTA. Using the *Escherichia coli* two-hybrid system and the phage display method, we identified galectin-2 as a binding partner of LTA. We purified the two recombinant proteins using a bacterial expression system, and confirmed direct binding of galectin-2 to LTA using an *in vitro* binding assay (Fig. 1a). We further examined their interaction in mammalian cells using constructs designed to express flag-tagged LTA or S-tagged galectin-2 and western blot analysis; co-immunoprecipitation of galectin-2 and LTA confirmed their interaction (Fig. 1b). Using antibodies specific to each protein, we also investigated subcellular localization of native galectin-2 and LTA in U937 cells, and found that these proteins co-localized in the cytoplasm (Fig. 1c).

We then examined whether any genetic variation in *LGALS2* was associated with susceptibility to MI. Re-sequencing the *LGALS2* genomic region using DNA from 32 MI samples revealed 17 additional single nucleotide polymorphisms (SNPs) (Fig. 2a). Next, we compared the genotype frequencies of approximately 600 individuals with MI, and 600 controls at these SNP loci, and found that one SNP (3279C \rightarrow T) in intron-1 of *LGALS2* was significantly associated with MI (designated SNP1 in Supplementary Table 1). This association was confirmed by increasing the number of samples to 2,302 for patients with MI and 2,038 for

controls, and by including another set of samples (Table 1 and Supplementary Table 2).

We also analysed linkage disequilibrium using a subset of markers with minor allele frequency of >0.20 , and investigated haplotype structure within the *LGALS2* region (Supplementary Table 3). This allowed us to identify a haplotype block containing three SNPs (SNP9, SNP10 and SNP11); no particular haplotype showed a higher statistical significance for association with MI than the single SNP alone (Supplementary Table 4). Because the minor allele frequency of the associated SNP was lower in the patients' group (Table 1), we concluded from these genetic studies that the minor variant protects against the risk of MI, although our study included only Japanese subjects and so its relevance to other populations remains to be clarified.

To investigate the biological significance of this genetic variation in intron-1 of *LGALS2*, we constructed reporter plasmids with a genomic fragment containing the SNP downstream of a luciferase gene and the SV40 enhancer sequence, and examined the effect of the intron-1 SNP on gene expression. The clone containing the 3279T allele showed nearly 50% less transcriptional activity than those containing the 3279C allele or the vector alone (Fig. 2b, c). These observations indicated that the nucleotide substitution could potentially reduce the level of intracellular galectin-2.

We then hypothesized that the amount of intracellular galectin-2 might regulate the extracellular secretion level of LTA, thereby influencing the degree of inflammation. To test this hypothesis, we examined the effect of the level of galectin-2 on the secreted level of LTA in the medium by repressing galectin-2 expression using a small interference (si)RNA technique, and by over-expressing

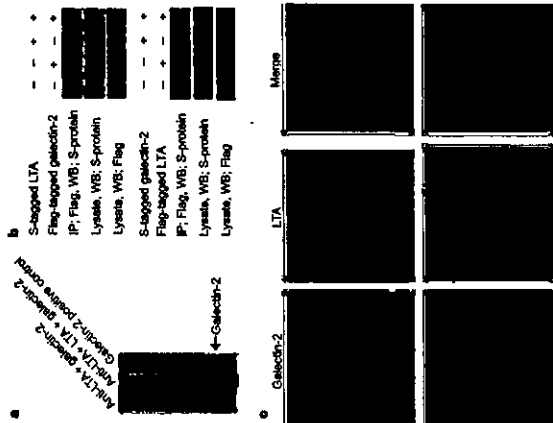


Figure 1 LTA binds to galectin-2. a, *In vitro* binding assay. b, Co-immunoprecipitation of tagged LTA and galectin-2 in U937 cells. c, Co-localization of endogenous LTA with galectin-2 in U937 cells (top row) with enlarged images of representative cells in the upper panels (bottom row). P, immunoprecipitation; WB, western blot.

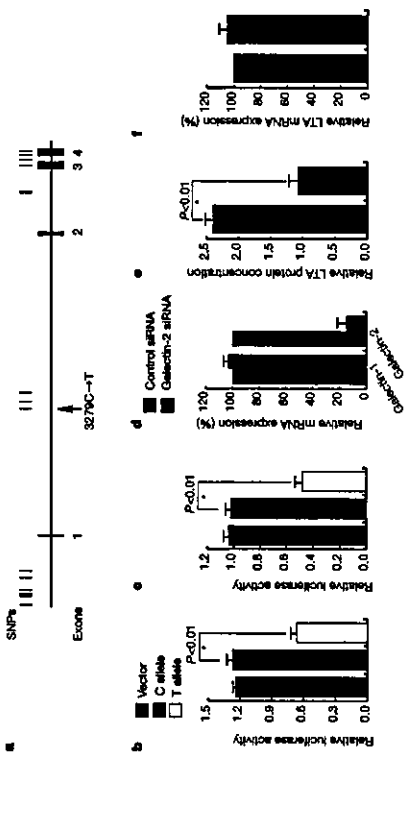


Figure 2 Association of a SNP in *LGALS2* with myocardial infarction and its functionality. a, Map of SNPs in *LGALS2* locus. b, c, Transcriptional regulatory activity of intron-1 SNP of *LGALS2* in HeLa (b) and HepG2 (c) cells. d, e, Inhibition of galectin-2 expression. Levels of *LGALS2* in HeLa (d) and HepG2 (e) cells. f, Inhibition of galectin-2 expression. Levels of galectin-1 or galectin-2 mRNA (f), secretant LTA protein (g), and LTA mRNA (h) after 48 h transfection with siRNA vectors. Students' *t*-test. Each experiment was repeated three times and each sample was studied in triplicate.

galectin-2. One siRNA for galectin-2 repressed galectin-2 messenger RNA to nearly one-fifth of its original level (Fig. 2d) and resulted in inhibition of LTA secretion into the medium (Fig. 2e). Over-expression of galectin-2 enhanced LTA secretion (Supplementary Fig. 1a). As shown in Fig. 2f, the LTA mRNA level was unchanged by knockdown or over-expression of galectin-2 (see also Supplementary Fig. 1b).

To further investigate the regulatory mechanism of LTA secretion by galectin-2, we searched for intracellular molecules that associate with galectin-2, using a tandem affinity purification (TAP) system. We identified two unique bands that could be observed only when the galectin-2-TAP tag was expressed (Fig. 3a). On the basis of a MALDI/TOF (matrix-assisted laser desorption/ionization-time-of-flight) mass spectrometry analysis, these two bands were shown to correspond to α - and β -tubulin—important components of microtubules. Using HeLa cells transfected with a plasmid to express flag-tagged galectin-2, we confirmed co-immunoprecipitation of endogenous tubulins and galectin-2 (Fig. 3b and data not shown). Interestingly, the tubulins were also co-immunoprecipitated with LTA (Fig. 3b and data not shown). Images from serial confocal sections of double-immunostained U937 cells revealed

that galectin-2 and α -tubulin co-localized as reticular filamentous networks developed in the cytoplasm (Fig. 3c). Recently, microtubule cytoskeleton networks have been implicated in the subcellular transport of some proteins, including glucose transporter isoform (GLUT4) or thiamine transporter (THTR1)¹⁴. It is likely that LTA is another molecule that uses the microtubule cytoskeleton network for translocation. It is also conceivable that galectin-2 has a role in intracellular trafficking, although the precise role of galectin-2 in this trafficking machinery complex has yet to be elucidated.

To examine whether these proteins are expressed in the lesion of MI—that is, in atherosclerotic lesions of the coronary artery—and if so, to investigate in which part of the lesion they are expressed, we performed immunohistochemical staining of human coronary atherosclerotic specimens with anti-LTA or anti-galectin-2 antibody. As shown in Fig. 4a, b, immunoreactivities for both LTA and galectin-2 were detected in intimal cells in atherosclerotic plaques, some of which were spindle-shaped or contained vacuolated, round cytoplasm. Immunostaining of adjacent sections with anti-smooth muscle cell (SMC) α -actin or anti-CD68 showed that the majority of these cells were either SMCs or SMC-derived foam cells, with

Table 1 Association between MI and intron-1 SNP in *LGALS2*

Genotype	Number of patients with MI	Number of controls	Number of controls (%)
<i>LGALS2</i> Intron-1 3279C \rightarrow T			
CC	1,077	866	43.0
CT	1,014	903	44.9
TT	211	279	13.7
Total	2,302	2,038	100.0

	χ^2	P value	Odds ratio	95% CI
Genotype frequency	26.2	0.0000034	1.23	1.13–1.36
Allele frequency	21.1	0.0000546	1.21	1.06–1.37
CC versus others	10.0	0.0016	1.27	1.07–1.50
TT versus others	22.1	0.0000208	0.81	0.70–0.94

Nucleotide numbering is according to the relation nucleotide¹. CI, confidence interval.

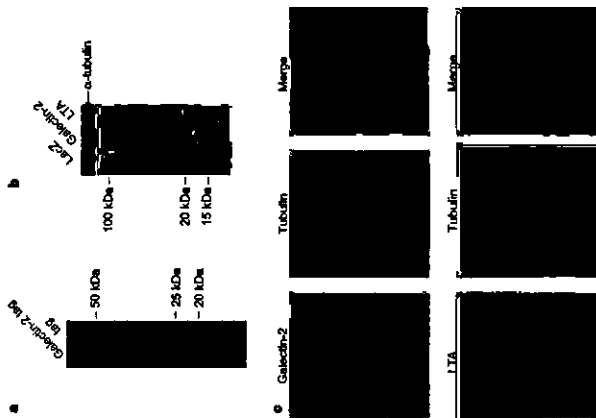


Figure 3 Gαi2-2 interacts with microtubules. **a**, Isolation of 1AP-tagged gαi2-2 and interacting proteins. Arrowheads indicate α- and β-tubulins, revealed by MALDI/TOF mass spectrometry analysis. **b**, Co-immunoprecipitation of endogenous α-tubulin with Flag-tagged gαi2-2 or CIA. Immunoprecipitations were done using anti-Flag M2 agarose, and immunoprecipitates were detected using anti-α-tubulin antibody (upper panel) or anti-Flag antibody (lower panel). Flag-tagged LacZ encoding β-galactosidase was used as a negative control. **c**, Co-localization of endogenous α-tubulin with endogenous gαi2-2 or LTA in U937 cells.

occasional macrophages being observed (Fig. 4c, d and Supplementary Fig. 2). Co-expression of LTA and gαi2-2 was also observed in the majority of polymorphic SMCs by double-labelled immunohistochemistry (Fig. 4e). In contrast, expression of either protein was not detectable in atrophic SMCs of fibrous plaques with scanty cellularity or in normal medial SMCs (Fig. 4f for LTA; data not shown for gαi2-2).

These results showed that LTA and gαi2-2 were co-expressed in SMCs and macrophages in the intima of human atherosclerotic plaques, but were absent in quiescent or normal medial SMCs. We also confirmed their co-expression by counting immunohistochemically double-labelled cells (Supplementary Table 5). A recent report also indicated that LTA was expressed in atherosclerotic lesions in mice and that loss of LTA reduced the size of the lesions¹⁷. Together, these results indicate that LTA, as one of the mediators of inflammation, along with gαi2-2, as a regulator of LTA secretion might have roles in the pathogenesis of MI, although the functional correlation of gαi2-2 and LTA with the development, progression or rupture of atherosclerotic plaques has yet to be clarified. We have identified gαi2-2 as another risk factor for MI. We believe that the results of this study provide an anchoring point for better understanding of the pathogenesis of MI. □



Figure 4 Expression and co-localization of gαi2-2 and LTA in the coronary atherosclerotic lesions. Single-labelled immunohistochemistry of serial sections of primary atherosclerotic lesions from human coronary arteries obtained by fractional coronary atherectomy, stained with anti-human LTA (a), anti-human gαi2-2 (b), monoclonal anti-SMO α-actin (c), and monoclonal anti-C268 (d). Magnification, ×100. **e**, Double-labelled immunohistochemical staining with anti-LTA (brown) and gαi2-2 (blue) antibodies. Magnification, ×119. **f**, Single-labelled immunohistochemical staining with anti-human LTA for atrophic SMCs of fibrous plaques with scanty cellularity and normal medial SMCs. Magnification, ×100.

Methods

DNA samples

The study included 1,638 Japanese patients with MI, referred to as the Osaka Acute Coronary Intervention Study (OACSIS) group. The diagnosis of definite MI has been described previously¹⁸. The control subjects consisted of 2,497 general populations recruited through several medical facilities in Japan. All subjects were genotyped for the polymorphic SNPs in the LTA gene, and their genotypes were confirmed by the genotyping of the Osaka Academic SNR Research Center. The Institute of Physical and Chemical Research (RIKEN), Yokohama.

SNP analysis

Design for polymorphic toxin reaction (PCR) primers, PCR experiments, DNA extraction, DNA sequencing, SNP discovery, genotyping of SNPs and statistical analysis has been described previously¹⁸.

LacZ two-hybrid and phage display screening

We constructed a two-hybrid complementary DNA (cDNA) library using mRNA isolated from human cells (RIKEN Cell Bank; RC30966) and *Saccharomyces cerevisiae* two-hybrid system library construction kit (Clontech), and screened the library using pBT-LacZ library as bait. For the phage display system, we constructed a phage display cDNA library using mRNA isolated from human cells and T7 phage display system (Novogen). We screened the library using the immobilized LTA as the bait.

Tandem affinity purification

The tandem affinity purification procedure was carried out essentially as described in ref. 4, with some modifications. We constructed a fusion cassette encoding a His tag, a V5EY cleavage site, and an S tag as a 2N tag sequence in pCMV-His vector (Sigma). The 2N tag in mammalian cells under the control of cytomegalovirus promoter. The 2N tag vector was transfected into HEK293 cells. The His tag and S tag were detected by Western blotting (USBAB; C2H3090A). The protein bands were analysed by MALDI/TOF mass spectrometry at AFRO Life Science.

In vitro binding assay and co-immunoprecipitation experiment

We prepared purified 3-tagged recombinant LTA and T7-tagged gαi2-2 derived from *E. coli* using the pET system (Novogen), and combined them. The co-immunoprecipitation experiments were performed using a monoclonal antibody against LTA (RAD System) coupled to HiTrapTM NHS-activated Sepharose HP (Amersham). We visualized the immune complex using 17 tag antibody (Stratagene) and horseradish peroxidase (HRP) conjugated with anti-mouse IgG antibody. For co-immunoprecipitation in mammalian cells, we transfected expression plasmids of Flag or 3-tagged LTA, gαi2-2 and LacZ (as a negative control) into COS7 cells (HSROR; PC93B17) or HeLa cells using Lipofectamine (Invitrogen) (see below). Twenty-four hours after transfection, cells were lysed, and immunoprecipitations were performed using anti-Flag tag M2 agarose (Kodak) and immunoprecipitates were detected using anti-Flag tag M2 agarose (Kodak) and immunoprecipitates were detected using anti-Flag tag M2 agarose (Kodak) and immunoprecipitates were detected using anti-Flag tag M2 agarose (Kodak) and immunoprecipitates were detected using anti-Flag tag M2 agarose (Kodak).

Cofactor immunology

Polyclonal anti-human gαi2-2 antibodies were raised in rabbits using recombinant protein synthesized in *E. coli*. The antisera showed no cross-reactivity to structurally related molecular gαi2-1 and gαi2-3, analysed by western blot. Polyclonal anti-gαi2-2 antisera and other goat anti-human LTA IgG (RAD System) or mouse anti-human α-tubulin monoclonal (αM) antibodies were used with Alexa secondary antibodies (Molecular Probes). U937 cells (HSROR; PC93B17) were stimulated for 30 min with phorbol myristate acetate (PMA) (20 ng ml⁻¹) and fixed. They were subsequently incubated with the corresponding primary antibodies in phosphate-buffered saline containing 1% bovine serum albumin, and the corresponding Alexa secondary antibodies.

siRNA and over-expression experiments

The target sequences for gαi2-2 (5'-ATCCAGCATGTCGACTCT-3') were cloned into pSilencer 2A1A siRNA vector (Ambion). For the over-expression experiment, the gαi2-2 was cloned into pFlag-CMV2A vector. After transfection, Jurkat cells were stimulated with PMA (20 ng ml⁻¹) for 24 h, and cells and supernatants were collected separately. LTA concentration was measured using an LTA-specific ELISA system (RAD System), and normalized by comparison with total protein concentration. The mRNA quantification procedure has been described previously¹⁸.

Luciferase assay

ADNA fragment, corresponding to nucleotides 5,188 to 5,404 of factor-1 of EGAL2, was cloned into pGL3-enhancer vector (Promega). In the downstream of SV40 enhancer in the 5' to 3' orientation. After 24 h transfection, luciferase activity was measured using the Dual-Luciferase Reporter Assay System (Promega).

Immunohistochemistry

Tissue samples were obtained from 16 patients with MI by elective surgical coronary artery bypass grafting. The samples were fixed with 4% paraformaldehyde and embedded in paraffin. Serial sections (5 μm) were stained with haematoxylin and eosin (H&E) and immunohistochemically stained with anti-human gαi2-2 antibody. Staining of adjacent sections was carried out using haematoxylin-eosin (H&E) or anti-human LTA IgG (RAD System) and rabbit polyclonal anti-gαi2-2 antibody. Staining of adjacent sections was carried out using haematoxylin-eosin (H&E) or anti-human LTA IgG (RAD System) and rabbit polyclonal anti-gαi2-2 antibody. Staining of adjacent sections was carried out using haematoxylin-eosin (H&E) or anti-human LTA IgG (RAD System) and rabbit polyclonal anti-gαi2-2 antibody.

Statistical analysis

Statistical analysis was performed using the Fisher's exact test. The results are expressed as mean ± s.d. unless otherwise indicated. Statistical significance was determined by the Fisher's exact test. P < 0.05 was considered significant.

11. Mizumi, M. et al. Expression of SN-PROX, a novel cell surface scavenger receptor for phospholipid-lysine and oxidized LDL, in human atherosclerotic lesions. *Atherosclerosis* **176**, 211-219 (2001).
12. Shi, S. L., Li, M. & Kahn, K. L. Angiogenin is a novel endothelial cell growth factor: its role in angiogenesis and its inhibition by endostatin. *Proc Natl Acad Sci USA* **97**, 741-746 (1999).
13. Okamoto, T. & Okamoto, S. L. Molecular mechanisms of endothelial cell apoptosis and its regulation in atherosclerosis. *Circulation* **107**, 117-121 (2003).

Supplementary information accompanies this paper on www.nature.com/nature

Supplementary information is available for this article. To view supplementary information for this article, please refer to the supplementary information for this article. The authors declare that they have no competing financial interests.

Correspondence and requests for materials should be addressed to T.T.

(takahashi@nrc.riken.ac.jp).

Reprints and permissions information is available at www.nature.com/reprints

permissions

permissions

permissions

permissions

permissions

permissions

permissions

permissions

permissions

permissions

permissions

permissions

permissions

permissions

permissions

permissions

permissions

permissions

permissions

permissions

permissions

permissions

permissions

permissions

permissions

permissions

permissions

permissions

permissions

permissions

permissions

permissions

LIHIT LAB.
11-2025